Cluster Transfer Reactions between Complex Nuclei*

ARNON DAR
Department of Nuclear Physics, Weizmann Institute of Science, Rehovoth, Israel
(Received 18 January 1965)

Cluster transfer reactions between complex nuclei are discussed in a simple semiclassical approximation. For energies below the Coulomb barrier nuclear distortions are neglected, and the results coincide with the "tunneling model" predictions of Breit. For energies above the Coulomb barrier, distortions are taken into account by a finite-range diffraction model. Closed-form expressions are obtained for the angular distribution of the reaction products and for the transfer excitation function. Coulomb effects are shown to play a dominant role in determining the main features of the reaction. Good agreement with experimental data is obtained.

I. INTRODUCTION

IT was first emphasized by Breit and co-workers[1] that the theoretical description of heavy-ion processes is greatly simplified by the validity of the semiclassical approximation characterized by the condition of a large Coulomb parameter. This was extensively used by Breit and Ebel[1] in the "tunneling model" with its restricted applications (to single-neutron transfer and energies below the Coulomb barrier). However, most of the experimental data in nucleon transfer has been obtained at energies above the Coulomb barrier with the following typical features:

(a) A peak in the angular distribution is observed, whose height and width vary systematically with energy.

(b) The variation of the position of the peak with energy is found empirically to correspond, approximately, to a Rutherford scattering along a classical trajectory with constant distance of approach of the order of the sum of radii of the colliding particles.

(c) The transfer excitation function shows a slow increase with energy and eventually it levels off at higher energies.

The angular distribution in transfer reactions was given by Greider[2] whose approximation is valid[3] for situations wherein long-range forces are dominant. This author demonstrated the importance of absorption effects in transfer reactions between complex nuclei. However, the inclusion of these effects was by a simple Butler-type hole model which neglects the important shadowing effects.

Another approach has been developed recently by Frahn and Venter.[4] They treat cluster transfer reactions between complex nuclei as quasi-elastic processes in the framework of the strong-absorption model for nuclear scattering. Rather general assumptions about the form of the scattering function in l space led them to a closed-form expression for the angular distribution of the outgoing particles. There are two weak points in their treatment:

(1) Their arbitrary choice for the scattering function can be proved to hold only for collective excitations of complex nuclei via inelastic scattering, and quite a different form will be shown here to hold for nucleon transfer reactions.

(2) In its present form their treatment is applicable only in cases where the energy is well above the Coulomb barrier and where no angular momentum is transferred between the colliding particles.

An alternative approach is offered by the distorted-wave Born approximation (DWBA) procedure. However, for heavy projectiles the zero-range approximation is certainly unjustified and one has to carry out laborious finite-range calculations. Moreover, the typical feature of such reactions is the strong absorption which takes place at small impact parameters. This is taken into account in the DWBA by a large imaginary part in the optical potential, but doing this produces an extra reflection. Moreover, even if one accepts the general applicability of the DWBA treatment, it is so general and contains so many parameters that it is not easy to know whether agreement with experimental data (which is generally found sooner or later by adjusting the parameters) is really significant or not.

In order to overcome these difficulties we present here a simple semiclassical approach. Nuclear distortions of the incoming and outgoing waves are neglected for energies below the Coulomb barrier, and the results (simple closed-form expressions) coincide with the "tunneling model" predictions of Breit.[1] For ener-

* The research reported in this document has been sponsored in part by the National Bureau of Standards.

[1] (a) G. Breit, M. H. Hu, Jr., and R. L. Gluckstern, Phys. Rev. **104**, 1030 (1956). (b) G. Breit and M. E. Ebel, Phys. Rev. **103**, 679 (1956); **104**, 1030 (1956). (c) G. Breit, *Encyclopedia of Physics* (Springer-Verlag, Berlin, 1959), 41/1, Sec. 48, p. 367. (d) G. Breit in *Proceedings of the Second Conference on Reactions between Complex Nuclei, 1960*, edited by A. Zucker *et al.* (John Wiley & Sons, Inc., New York, 1960), p. 1. (e) G. Breit, *Proceedings of the Conference on Direct Interactions and Nuclear Reaction Mechanism* (Gordon and Breach Publishers, Inc., New York, 1962), p. 480. (f) G. Breit, *Proceedings of the 3rd Conference on Reactions between Complex Nuclei* (University of California Press, Berkeley, 1963), p. 97.

[2] K. R. Greider, Ref. 1(f), p. 148; Ref. 1(e), p. 971; Phys. Rev. Letters **9**, 392 (1962); Phys. Rev. **133**, B1483 (1964).

[3] See however, L. J. Goldfarb and P. J. A. Buttle, Phys. Letters **11**, 54 (1964).

[4] W. E. Frahn and R. H. Venter, Slellenbosch University, 1964 (unpublished).

gies above the Coulomb barrier, distortions are taken into account by a finite-range diffraction model. Closed-form expressions are obtained for the angular distribution of the reaction products and for the transfer excitation function under the following conditions:

(1) The Q value of the reaction is small compared with the incident energy.

(2) The mass transferred is small compared with the masses of the colliding particles.

(3) The angular momentum transferred is small compared with the dominant contributing l values.

(4) The value of the Coulomb parameter η is large so that the semiclassical condition $2\pi\eta \gg 1$ is well satisfied.

Under these conditions the particles move semiclassically in Rutherford trajectories which are not appreciably affected by the transfer of mass, energy, and angular momentum during the collision. They are especially well satisfied in neutron transfer reactions between complex nuclei.

Section II outlines the model. Closed-form expressions for the differential cross section and for the transfer excitation function are derived in Sec. III. In Sec. IV the predictions of the model are compared with experimental data. Conclusions are drawn in Sec. V.

II. THE DIFFRACTION MODEL

The simple diffraction approach to nuclear reactions[5] assumes that the exit channel in reactions, dominated by strong absorption in both the entrance and exit channels, is fed by encounters on a well-defined ring located around the target nucleus. This is based on the assumption that all smaller impact parameter collisions are completely exhausted by highly inelastic reactions, while the exponential decrease of the bound-state nuclear wave functions outside the nucleus restricts the reaction to the nuclear surface. Now, in Rutherford scattering an apsidal distance D is related to a c.m. scattering angle θ by

$$D=(\eta/k)[1+\csc(\theta/2)], \tag{1}$$

where

$$\eta=(mZ_aZ_Ae^2)/(\hbar^2k). \tag{2}$$

m is reduced mass of the colliding particles, Z_a and Z_A are the atomic numbers of projectile and target, respectively, and k is the wave number of their relative motion. Therefore, if the reaction takes place on a well-defined ring with radius R, and if the colliding nuclei move along classical Coulomb trajectories which are not appreciably affected by the transfer, then one expects the angular distribution pattern to be peaked at an angle θ_0 which is given by

$$R_{aA}=(\eta/k)[1+\csc(\tfrac{1}{2}\theta_0)], \tag{3}$$

where

$$R_{aA}=r_0(A_a^{1/3}+A_A^{1/3}), \tag{4}$$

A_a and A_A being the mass numbers of the projectile a and the target A, respectively, and r_0 the nuclear radius constant.

This simple model involves several assumptions that might seem to make its validity questionable. For instance, the forward-angle approximation breaks time reversal invariance and limits the applicability of the model to small scattering angles; the exchange interaction is surely not concentrated on a well-defined ring; Coulomb effects are neglected, etc. A way to remove part of these difficulties was proposed by Henley and Yu[6] and by Dar.[7] However, in contrast with these references which are mainly concerned with the situation where Coulomb effects are negligible, we are now concerned with circumstances where they play a dominant role.

The natural extension of the earlier diffraction-model prescription is to calculate transition amplitudes in the Coulomb-wave Born approximation with the neglect of both the contributions from the absorption region and the shadow of the absorptive sphere. This is a sharp cutoff procedure (sharp boundaries for the absorptive sphere and shadow geometry in R space). However, the impressive improvement of the smooth cutoff procedure over the sharp one achieved by Blair *et al.*[8] and by Austern[9] in interpreting the elastic and inelastic scattering of medium-energy alpha particles, suggests that similar effects should be looked for in our case.

A smooth cutoff rather than a sharp one can be introduced in a way first proposed by Sopkovich[10] and rederived independently by Gottfried and Jackson[11] and by Durand and Chiu.[12] Following these authors one uses the partial-wave decomposition of the transition amplitude in the Coulomb-wave Born approximation, and instead of neglecting the low partial waves, which correspond to a small impact parameter, the amplitude of each partial wave is multiplied by the square root of its reflection coefficient a_l. ($\sqrt{a_l}=e^{i\delta_l}$, where δ_l is the phase shift of the lth partial wave.) Such a prescription is based on a WKB picture for

[5] A. Dar, Phys. Letters **7**, 339 (1963); Nucl. Phys. **55**, 305 (1964).

[6] E. M. Henley and D. U. L. Yu, Phys. Rev. **133**, B1445 (1964); **135**, B1152 (1964).

[7] A. Dar, Proceedings of the Paris Conference on Nuclear Physics, 1964 (unpublished).

[8] J. S. Blair, D. Sharp, and L. Wilets, Phys. Rev. **125**, 1625 (1962).

[9] N. Austern, Ann. Phys. **15**, 229 (1961); E. Rost and N. Austern, Phys. Rev. **120**, 1375 (1959).

[10] N. J. Sopkovich, Nuovo Cimento **26**, 186 (1962).

[11] K. Gottfried and D. Jackson, Nuovo Cimento **34**, 735 (1964).

[12] L. Durand, III and Yam Tsi Chiu (Lectures presented by L. Durand at the Boulder Conference on Particle Physics, 1964) (unpublished); Yale University, July 1964 (unpublished).

direct reactions, and it may be interpreted as an interpolating procedure for the DWBA.

In Sec. III we apply this prescription to the calculation of the transition amplitude for cluster transfer reactions between complex nuclei.

III. THE DIFFERENTIAL CROSS SECTION AND THE TRANSFER EXCITATION FUNCTION

In the Coulomb-wave Born approximation the transition amplitude is computed as a first-order matrix element between channel wave functions for the colliding systems A, a and the separating systems B, b. That is, the transition amplitude for the reaction $A(a,b)B$ has the form of a matrix element between product wave functions

$$T_{ba}=(\Psi_B\Psi_b\chi_b^{(-)}(\mathbf{k}_b,\mathbf{r}_b),V\Psi_A\Psi_a\chi_a^{(+)}(\mathbf{k}_a,\mathbf{r}_a)). \quad (5)$$

Here Ψ_B, Ψ_b, Ψ_A, Ψ_a are the internal wave functions for the noninteracting separated particles B,b,A,a. The interaction V is the interaction whose off-diagonal matrix elements are responsible for the transition. $\chi_b^{(-)}$ and $\chi_a^{(+)}$ are the Coulomb waves for the elastic-scattering wave functions of the pairs A,a and B,b, respectively.

Equation (5) may be written in the form

$$T_{ba}=\int d\mathbf{r}_a\int d\mathbf{r}_b\chi_b^{(-)*}(\mathbf{k}_b,\mathbf{r}_b) \times\langle B,b|V|a,A\rangle\chi_a^{(+)}(\mathbf{k}_a,\mathbf{r}_a), \quad (6)$$

with

$$\langle B,b|V|a,A\rangle=\int\Psi_B^*\Psi_b^*V\Psi_A\Psi_a d\xi, \quad (7)$$

where ξ represents all the coordinates other than $\mathbf{r}_a$ and $\mathbf{r}_b$. The last matrix element plays the role of an effective interaction or form factor, for the transition between the elastic scattering states $\chi_a^{(+)}$, $\chi_b^{(-)}$. For cluster transfer reactions, a is assumed to form a bound state of b and c, while B is assumed to form a bound state of A and c, i.e., the reaction is described symbolically as

$$A+a\rightarrow B+b\equiv A+(c+b)\rightarrow(A+c)+b,$$

where closed parentheses denote bound states. V is taken to be the interaction between b and c. In the projectile a, the clusters b and c are taken to be in a relative state with a definite orbital angular momentum l_a, while c is assumed to be captured by A into a state with a definite angular momentum l_c. We denote by j_i, l_i, and J_i the spin, orbital, and total angular momentum of particle i, respectively, and by m_i, μ_i, and M_i, the corresponding magnetic quantum numbers. For the overlap integral $\langle B|A\rangle$ of the target and final nucleus present in Eq. (7), we take a bound-state wave function for particle c in the central field of the target nucleus with quantum numbers l_c, j_c, μ_c, m_c. The radial and angular parts of the wave function are u_{l_c}, Y_{l_c}, respectively. If we further assume no coupling between orbital and spin parts, then the approximations described above lead to an effective interaction of the form

$$\langle B,b|V|a,A\rangle=\sum_{m_b,m_c,\mu_c,M_c}(j_cm_cl_c\mu_c|J_cM_c) \times(j_cm_cl_a\mu_a|J_c'M_c')(J_cM_cJ_AM_A|J_BM_B) \times(j_bm_bJ_c'M_c'|J_aM_a)F_{\mu_a\mu_c}. \quad (8)$$

Here

$$F_{\mu_a\mu_c}=\langle U_{l_c}(r_c)Y_{l_c\mu_c}(\Omega_c)|V(r_{bc})|\chi_{l_a}(\mathbf{r}_{bc})\rangle, \quad (9)$$

where χ_{l_a} is the internal wave function describing the relative motion of b and c inside particle a. The diffraction model assumes that the reaction takes place mainly outside the nucleus where

$$U_{l_c}(r_c)\sim Ce^{-\beta r_c}/(\beta r_c). \quad (10)$$

β is related to the binding energy $-\epsilon_B$, of c in B through

$$\epsilon_B=(\hbar^2\beta^2)/(2M_{cA}), \quad (11)$$

with M_{cA} the reduced mass of particles A and c. C is a normalization constant.

According to the diffraction picture the reaction is most probable for a grazing collision such that the centers of masses of the colliding particles and that of the transferred particle are lying all along the same straight line with the transferred particle in the middle. For such a situation we can use the expansion:

$$\frac{Ce^{-\beta|\mathbf{r}_b-\mathbf{r}_{bc}|}}{\beta|\mathbf{r}_b-\mathbf{r}_{bc}|}Y_{l_c\mu_c}(\Omega_c)\sim-4\pi CY_{l_c\mu_c}(\Omega_b) \times\sum_{l=0}^{\infty}\sum_{m=-l}^{l}j_l(i\beta r_{bc})h_l(i\beta r_b)Y_{lm}(\Omega_b)Y_{lm}^*(\Omega_{bc}), \quad (12)$$

where j_l and h_l are the spherical Bessel and Hankel functions, respectively.

We now introduce Eq. (12) into Eq. (9). Due to the orthogonality of the spherical harmonics, only the term with $(l,m)=(l_a,\mu_a)$ in Eq. (12) contributes, and the form factor F_{μ_c} reduces to the form

$$F_{\mu_a\mu_c}=-C(4\pi)^{1/2}\int j_{l_a}(i\beta r)V(r)\chi_{l_a}(r)r^2dr \times h_{l_a}(i\beta r_b)Y_{l_a\mu_a}(\Omega_b)\times Y_{l_c\mu_c}(\Omega_b). \quad (13)$$

Next we introduce Eqs. (8), (13) into Eq. (5) and approximate $\chi_a^{(+)}(\mathbf{k}_a,\mathbf{r}_a)$ by $\chi_a^{(+)}(\mathbf{k}_a,\mathbf{r}_b)$, which amounts to the replacement of the c.m. coordinate of particle $(b+c)$ by the c.m. coordinate of particle b. This approximation is expected to be accurate enough under condition 2.

Using the saddle-point approximation[13,14] and the

[13] K. Ter Martirosian, Zh. Eksperim. i Teor. Fiz. **29**, 620 (1955) [English transl.: Soviet Phys.—JETP **2**, 620 (1956)].

[14] A. Dar, A. de-Shalit, and A. S. Reiner, Phys. Rev. **131**, 1732 (1963).

orthogonality relations of the Clebsch-Gordan coefficients, the differential cross section may be easily shown to be given by

$$\frac{d\sigma}{d\Omega}=\frac{M_{bB}M_{aA}}{(2\pi\hbar^2)^2}\left(\frac{k_b}{k_a}\right)\frac{(2J_B+1)}{(2J_A+1)}|F|^2|B_{l_a}|^2, \quad (14)$$

where

$$F=-(4\pi)^{1/2}\int j_{l_a}(i\beta r)V(r)\chi_{l_a}(r)r^2dr \quad (15)$$

and

$$B_{l_a}=C\int \chi_b^{(-)}(\mathbf{k}_b,\mathbf{r})^*h_{l_a}(i\beta r)\chi_a^{(+)}(\mathbf{k}_a,\mathbf{r})d\mathbf{r}. \quad (16)$$

Next we turn to the orbital integral $B_{l_a}(\theta)$, using partial-wave expansion, i.e.,

$$\chi^{(\pm)}(\mathbf{k},\mathbf{r})=\sum_{l,m}4\pi(-1)^m i^l e^{\pm i\sigma_l}Y_{l-m}(\mathbf{k}) \times Y_{l,m}(\theta,\phi)\frac{F_l(kr)}{kr}. \quad (17)$$

Here F_l are the radial Coulomb wave functions and σ_l are the Coulomb phase shifts given by

$$e^{2i\sigma_l(\eta)}=\frac{\Gamma(l+\frac{1}{2}+i\eta)}{\Gamma(l+\frac{1}{2}-i\eta)}. \quad (18)$$

The orbital integrals B_{l_a} then reduce to the form:

$$B_{l_a}(\theta)=(4\pi)^{1/2}\sum_l(2l+1)e^{2i\sigma_l}I_l^{l_a}P_l(\cos\theta), \quad (19)$$

where

$$\cos\theta=(\mathbf{k}_a\cdot\mathbf{k}_b)/k_ak_b \quad (20)$$

and

$$I_l^{l_a}=\frac{C}{k_ak_b}\int_0^\infty F_l(k_br)h_{l_a}(i\beta r)F_l(k_ar)dr. \quad (21)$$

According to the diffraction model prescription one has now to multiply the summand in Eq. (19) by $\bar{a}_l$. We therefore replace $B_{l_a}(\theta)$ by $\bar{B}_{l_a}(\theta)$ where

$$\bar{B}_{l_a}(\theta)=(4\pi)^{1/2}\sum(2l+1)\bar{a}_le^{2i\sigma_l}I_l^{l_a}P_l(\cos\theta), \quad (22)$$

where

$$\bar{a}_l=[a_l(a)a_l(b)]^{1/2}. \quad (23)$$

The differences between the elastic scattering in the entrance and exit channel have been neglected in Eqs. (19), (22). This is justified under conditions 1–4. For large values of l or for energies below the Coulomb barrier the difference between $I_l^{l_a}$ and I_l^0 is negligible. The I_l^0 integrals can be evaluated explicitly but their result is very cumbersome. Rather, we follow Lemmer[15] who, for large Coulomb parameter, replaced the radial Coulomb functions by their classical counterparts as obtained from WKB calculations.[16] The radial integrals are then quite simple to evaluate. We shall only outline here the procedure. More details are found in Refs. 1(c), 15, 16. Using the WKB forms for $F_l(k_ar)$ and $F_l(k_br)$ and changing variables from r to ω where $kr=\eta(1+\epsilon\cosh\omega)$, one has

$$I_l^0=\frac{Ce^{-\gamma}}{4\beta\bar{k}^2}\int_{-\infty}^{+\infty}\exp(i\xi\omega+i\xi\sinh\omega-\gamma\epsilon\cosh\omega)d\omega \quad (24)$$

for the radial integrals.

The constants appearing in this expression are defined as follows: Let η_a and η_b be the values of the Coulomb parameter in the entrance and exit channel, respectively, and let $\bar{\eta}$ be their average; then $\xi=\eta_a-\eta_b$ and $\gamma=\bar{\eta}\beta/\bar{k}$ where $\bar{k}$ is the average wave number. The constant ϵ is the eccentricity of the hyperbolic orbit of a charged particle moving in a Coulomb field with $\eta=\bar{\eta}$ and angular momentum l.

$$\epsilon=[\bar{\eta}^2+l(l+1)]^{1/2}/\bar{\eta}. \quad (25)$$

Such an orbit can be roughly regarded as a smooth average orbit of the incident and outgoing particles in the Coulomb field of the target nucleus. This approximation may be justified by noting that the energy and mass transferred in the reactions are small compared to the kinetic energy and masses of the colliding particles, respectively. A change of variables transforms I_l^0 into a representation of a Bessel function of the second kind and of an imaginary order

$$I_l^0=(Ce^{-\gamma}/2\beta\bar{k}^2)\exp(-\xi\phi)K_{i\xi}[(\gamma^2+\xi^2)^{1/2}\epsilon], \quad (26)$$

with

$$\tan\phi=\xi/\gamma.$$

For large values of the argument we can approximate I_l^0 by

$$I_l^0\sim\frac{Ce^{-\gamma-\xi\phi}}{2\beta\bar{k}^2}\left[\frac{\pi\eta}{2(\gamma^2+\xi^2)^{1/2}}\right]^{1/2}\frac{1}{[l(l+1)+\bar{\eta}^2]^{1/4}} \times\exp[-(\gamma^2+\xi^2)^{1/2}[l(l+1)+\bar{\eta}^2]^{1/2}/\bar{\eta}]. \quad (27)$$

A. Energy below the Coulomb Barrier

Let us first treat the case of energies below the Coulomb barrier.

(a) *The Differential Cross Section*

We note that for energy well below the Coulomb barrier $a_l\equiv 1$. Then, to perform the l summation in Eq. (22) we note that its phase is stationary only at

$$l_\theta\sim\bar{\eta}\cot(\tfrac{1}{2}\theta). \quad (28)$$

As a result the I_l factor only contributes appreciably

[15] R. Lemmer, Nucl. Phys. **39**, 680 (1962).

[16] K. Alder, A. Bohr, T. Huss, B. Mottelson, and A. Winther, Rev. Mod. Phys. **28**, 432 (1956).

at $l\sim l_\theta$ and we can take it outside the sum in order to obtain

$$\bar{B}_{l_a}(\theta)\approx B(\theta)=\frac{(4\pi)^{1/2}ce^{-\gamma-\xi\phi}}{2\beta\bar{k}^2}\left[\frac{\pi\sin(\frac{1}{2}\theta)}{2(\gamma^2+\xi^2)^{1/2}}\right]^{1/2}\times\exp[-(\gamma^2+\xi^2)^{1/2}\csc(\tfrac{1}{2}\theta)]\times\sum(2l+1)e^{2i\sigma_l}P_l(\cos\theta). \quad (29)$$

The sum on the right-hand side of Eq. (29) is proportional to the Rutherford amplitude $f_c(\theta)$.

$$f_c(\theta)=\{\bar{\eta}/[2k(\sin\tfrac{1}{2}\theta)^2]\}\exp[-2i\eta\ln(\sin\tfrac{1}{2}\theta)+2i\sigma_0+i\pi]. \quad (30)$$

Substitution of (30) into (29) yields

$$|B(\theta)|^2=\frac{\pi^2\bar{\eta}^2c^2e^{-2\gamma-2\xi\phi}}{\beta^2\bar{k}^4(\gamma^2+\xi^2)^{1/2}}[\sin(\tfrac{1}{2}\theta)]^{-3}\times\exp[-2(\gamma^2+\xi^2)^{1/2}\csc(\tfrac{1}{2}\theta)]. \quad (31)$$

In the DWBA, the choice of V_{bc} or V_{Ac} for V in the calculation of the transition amplitude [Eq. (6)] is equally good. However, the choice of any one of them breaks time reversal. It may be restored by using an *ad hoc* assumption, namely: The transition amplitude is given by the geometrical average of those calculated with V_{bc} and V_{Ac}.

It is easy to show that, under this modification, $|B(\theta)|^2$ reads

$$|B(\theta)|^2\sim\frac{\pi^2\bar{\eta}^2c^2e^{-\gamma_1-\gamma_2-\xi\phi_1-\xi\phi_2}}{2\beta\times\alpha\bar{k}^4[(\gamma_1^2+\xi^2)(\gamma_2^2+\xi^2)]^{1/4}}[\sin(\tfrac{1}{2}\theta)]^{-3}\times\exp\{-[(\gamma_1^2+\xi^2)^{1/2}+(\gamma_2^2+\xi^2)^{1/2}]\csc(\tfrac{1}{2}\theta)\}, \quad (32)$$

where

$$\gamma_1=\bar{\eta}\beta/\bar{k},\qquad \gamma_2=\bar{\eta}\alpha/\bar{k},$$
$$\tan\phi_1=\xi/\gamma_1,\quad \tan\phi_2=\xi/\gamma_2. \quad (33)$$

α is related to the binding energy $-\epsilon_a$ of b and c in a through

$$\epsilon_a=(\hbar^2\alpha^2)/2M_{bc}. \quad (34)$$

(b) *The Apsidal Distance Distribution*

The tunneling model prediction for the angular distribution is

$$(d\sigma/d\Omega)\alpha[\sin(\tfrac{1}{2}\theta)]^{-3}\exp(-\alpha D-\beta\bar{D}), \quad (35)$$

where D and $\bar{D}$ are the apsidal distances for the delivering and accepting nucleus, respectively. Noting that

$$\frac{d\sigma}{dD}=\frac{-8\pi k}{\bar{\eta}}[\sin(\tfrac{1}{2}\theta)]^{-3}\frac{d\sigma}{d\Omega}, \quad (36)$$

one gets the tunneling-model prediction for the apsidal distance distribution

$$(d\sigma/dD)\alpha\exp(-\alpha D-\beta\bar{D}). \quad (37)$$

Now, for energy below the Coulomb barrier our prediction is [Eq. (32)].

$$(d\sigma/d\Omega)\alpha[\sin(\tfrac{1}{2}\theta)]^{-3}\exp\{-[(\gamma_1^2+\xi^2)^{1/2}+(\gamma_2^2+\xi^2)^{1/2}]\csc(\tfrac{1}{2}\theta)\}, \quad (38)$$

but under conditions 1–4, $(\xi^2+\gamma^2)^{1/2}\sim\gamma$ and from Eqs. (1) and (36) we get

$$(d\sigma/d\Omega)\alpha\exp[-\gamma_1\csc(\tfrac{1}{2}\theta)-\gamma_2\csc(\tfrac{1}{2}\theta)]=\exp(-\alpha D-\beta\bar{D}). \quad (39)$$

Thus, under conditions 1–4, the two predictions coincide.

(c) *The Transfer Excitation Function*

We proceed now by calculating the transfer excitation function

$$\sigma(E)=\int\frac{d\sigma}{d\Omega}d\Omega. \quad (40)$$

From Eqs. (14) and (22) one obtains

$$\sigma(E)=\frac{M_{aA}M_{bB}}{(2\pi\hbar^2)^2}\frac{(2J_B+1)}{(2J_A+1)}\frac{k_b}{k_a}|F|^2S(E), \quad (41)$$

where

$$S(E)=4\pi\sum(2l+1)|I_l|^2. \quad (42)$$

One may now introduce the asymptotic expression for I_l [Eq. (27)] and approximate the sum over angular momentum by integration over classical distance of closest approach, i.e.,

$$[\bar{\eta}^{+2}+l(l+1)]^{1/2}=\bar{k}D-\bar{\eta}, \quad (43)$$

$$(2l+1)dl\sim 2\bar{k}(\bar{k}D-\bar{\eta})dD, \quad (44)$$

$$S(E)\sim\frac{\pi c^2\bar{\eta}\exp[-2\xi\phi-2\gamma+2(\gamma^2+\xi^2)^{1/2}]}{4\beta^2\bar{k}^3(\gamma^2+\xi^2)^{1/2}}\times\int_{R_{\min}}^{\infty}\exp\left[-\frac{2(\gamma^2+\xi^2)^{1/2}\bar{k}}{\eta}D\right]dD. \quad (45)$$

Hence

$$S(E)=\frac{\pi^2c^2\eta^{-2}}{2\beta^2\bar{k}^4(\gamma^2+\xi^2)}\exp[-2\gamma+2(\gamma^2+\xi^2)^{1/2}-2\xi\phi]\times\exp\{-[2(\gamma^2+\xi^2)^{1/2}/\bar{\eta}]\bar{k}R_{\min}\}, \quad (46)$$

where

$$R_{\min}\sim(Z_aZ_Ae^2)/E. \quad (47)$$

For $\xi/\gamma\ll 1$ ($\phi=\arctan(\xi/\gamma)\approx\xi/\gamma$), $S(E)$ reduces to

$$S(E)\sim(\pi c^2)/(8\beta^4\bar{k}^2)\exp(-\xi^2/\gamma)\exp(-2\beta Z_aZ_Ae^2/E), \quad (48)$$

where

$$\xi \approx -\frac{\bar{\eta}Q}{2E^{1/2}(E+Q)^{1/2}}, \quad \gamma \approx \frac{Z_a Z_A e^2}{2E^{1/2}(E+Q)^{1/2}}\beta. \tag{49}$$

Time reversal may be restored again in order to obtain

$$S(E) \propto (1/E)\exp(-\xi^2/\gamma)\exp(-\alpha Z_a Z_A e^2/E_a - \beta Z_b Z_B e^2/E_b). \tag{50}$$

For $\xi^2/\gamma \ll 1$, the last expression coincides with the "tunneling-model" prediction.

(d) *The Form Factor F*

In order to demonstrate that the form factor does not contribute any energy-dependent factor we treat explicitly the important case of deuteron stripping.

Let us assume that $V(r)$ in Eq. (15) is given by a Hulthen potential

$$V(r) = (V_0 e^{-\mu r})/(1-e^{-\mu r}), \tag{51}$$

where V_0 is the depth parameter of the well and μ^{-1} is the range of the potential. The corresponding normalized S-state wave function is

$$\chi_0 = \left[\frac{2\alpha(\alpha+\mu)(2\alpha+\mu)}{\mu^2}\right]^{1/2} \frac{e^{-\alpha r}(1-e^{-\mu r})}{r}. \tag{52}$$

In Eq. (15) we need the product $V(r)\chi_0(r)$ which can be taken from the Schrödinger equation:

$$\frac{\hbar^2}{2M_{bc}}\left(\frac{d^2}{dr^2}-\alpha^2\right)[r\chi_0(r)] = V(r)[r\chi_0(r)]. \tag{53}$$

Substitution of (53) into (15) yields

$$F = \frac{-(8\pi\alpha)^{1/2}\hbar^2}{2M_{bc}} \frac{\Gamma^2[\Gamma(\Gamma+\alpha)]^{1/2}}{(\Gamma^2-\beta^2)(\Gamma-\alpha)}, \tag{54}$$

with $\Gamma=\alpha+\mu$. The zero-range form factor F_0 may be obtained by letting μ^{-1}, the range of the potential, tend to zero, i.e.,

$$F_0 = \lim_{\mu\to\infty} F = \frac{(8\pi\alpha)^{1/2}\hbar^2}{m}. \tag{55}$$

Both F and F_0 are energy-independent; however, in contrast to the zero-range form factor, the finite-range form factor depends on both binding energies (of the neutron in the deuteron and in the accepting nucleus) and it increases with the range of the binding potential.

B. Energy above the Coulomb Barrier

Let us now pass to reactions with energy above the Coulomb barrier. The data on medium-energy elastic scattering of heavy ions, on complex nuclei may be satisfactorily interpreted[17] assuming a Woods-Saxon form for the l dependence of the reflection coefficients, i.e.,

$$\begin{aligned} a_l &= \{1+\exp[(L_0-l)/\delta]\}^{-1}, \\ L_0 &= k\bar{R}_{aA}[1-(2\bar{\eta}/k\bar{R}_{aA})]^{1/2}, \\ \delta &= k\bar{d}[1-(\bar{\eta}/k\bar{R}_{aA})][1-(2\bar{\eta}/k\bar{R}_{aA})]^{-1/2}. \end{aligned} \tag{56}$$

$L_0\hbar$ is the angular momentum which corresponds to a grazing collision, $\bar{d}$ is a constant playing the role of the diffuseness in R space; L_0 satisfies

$$E = \frac{L_0(L_0+1)\hbar^2}{2M_{aA}R_{aA}^2} + \frac{Z_a Z_A e^2}{R_{aA}}. \tag{57}$$

(a) *The Differential Cross Section*

For the evaluation of the differential cross section we introduce the following additional approximations which are valid under conditions 1–4.

(1) For large l, and θ satisfying

$$\theta \gg (4l)^{-1}, \quad \pi-\theta \gg (4l)^{-1},$$

$P_l(\cos\theta)$ may be replaced by the leading term in its asymptotic expansion

$$P_l(\cos\theta) \sim [\pi(2l+1)\sin\theta]^{-1/2}[e^{i\pi/4}e^{-i(l+\frac{1}{2})\theta} + e^{-i\pi/4}e^{i(l+\frac{1}{2})\theta}]. \tag{58}$$

For $|l+i\eta|$ large

$$2[\sigma_l-\sigma_{1/2}] \sim \eta[-2\ln(\sin\tfrac{1}{2}\psi)+\psi\cot\tfrac{1}{2}\psi]-\pi/2. \tag{59}$$

$$\frac{2d\sigma_l}{dl} \sim \psi, \tag{60}$$

where

$$\psi = 2\tan^{-1}(\bar{\eta}/l), \quad 0 \leqslant \psi \leqslant \pi. \tag{61}$$

The angle ψ has a simple classical interpretation when lh is interpreted as the c.m. angular momentum. In this case, ψ is the c.m. angle through which the projectile will be scattered classically in the pure Coulomb field.

Because of the structure of the reflection coefficient and the radial integrals the major contribution to $\bar{B}_{l_a}(\theta)$ in Eq. (22) arises from values of l in a small region around L_0. As a result, the following approximations may be introduced:

(2) $$e^{2i\sigma_l} \sim \exp(2i\sigma_{L_0})e^{i\theta_0 x}, \tag{62}$$

where

$$\theta_0 = 2\tan^{-1}(\bar{\eta}/L_0), \quad x = l-L_0, \tag{63}$$

(3) For $L_0 \gg \bar{\eta}$

$$(l+\tfrac{1}{2})^{1/2}I_l \sim [L_0(L_0+1)+\bar{\eta}^{+2}]^{1/4}I_{L_0}e^{-\frac{1}{2}\Delta x}, \tag{64}$$

where

$$\frac{\Delta}{2} = \frac{L_0(\gamma^2+\xi^2)^{1/2}}{\bar{\eta}[L_0(L_0+1)+\bar{\eta}^2]^{1/2}} \sim \frac{\beta}{\bar{k}}. \tag{65}$$

Finally, we introduce Eqs. (58) and (65) into Eq.

[17] W. E. Frahn and R. H. Venter, Ann. Phys. 27, 401 (1964).

(22) and approximate the sum over l by an integration in order to obtain

$$B(\theta)\sim(2L_0+1)^{1/2}I_{L_0}e^{2i\sigma_{L_0}}\times\frac{2\pi\delta}{(\sin\theta)^{1/2}}\{e^{i[(L_0+\frac{1}{2})\theta-\pi/4]}\csc[\pi(\Delta/2)\delta-i\pi\delta(\theta+\theta_0)]$$
$$+e^{-i[(L_0+\frac{1}{2})\theta-\pi/4]}\csc[\pi(\Delta/2)\delta+i\pi\delta(\theta-\theta_0)]\},\quad(66)$$

and

$$|B(\theta)|^2\sim4(2L_0+1)I_{L_0}{}^2\pi^2\delta^2\frac{1}{\sin\theta}\Big[\frac{1}{\cosh^2[\delta\pi(\theta-\theta_0)]-\cos^2[\delta(\Delta/2)\pi]}+\frac{1}{\cosh^2[\delta\pi(\theta+\theta_0)]-\cos^2[\delta(\Delta/2)\pi]}$$
$$+\frac{\cos[(2L_0+1)\theta-\pi/2][\cosh(2\pi\delta\theta_0)-\cos(\pi\delta\Delta)\cosh(2\pi\delta\theta)]-\sin[(2L_0+1)\theta-\pi/2]\sin(\pi\delta\bar{\Delta})\sinh(2\pi\delta\theta)}{\{\cosh^2[\delta\pi(\theta+\theta_0)]-\cos^2[\delta(\Delta/2)\pi]\}\{\cosh^2[\delta\pi(\theta-\theta_0)]-\cos^2[\delta(\bar{\Delta}/2\pi]\}}\Big].$$
$$(67)$$

Time reversal may be restored by replacing β by the arithmetic average $\bar{\beta}=(\alpha+\beta)/2$; i.e., Δ is replaced by $\bar{\Delta}$ where

$$\bar{\Delta}\sim(\alpha+\beta)/\bar{k}.\quad(68)$$

The sharp-cutoff result[18] may be obtained by letting δ in Eq. (66) tend to zero.

$$\lim_{\delta\to0}B(\theta)\sim2(2L_0+1)^{1/2}I_{L_0}\frac{\exp(2i\sigma_{L_0})}{(\sin\theta)^{1/2}}$$
$$\times\Big\{\frac{e^{-i[(L_0+\frac{1}{2})\theta-\pi/4]}}{\Delta/2+i(\theta-\theta_0)}+\frac{e^{+i[(L_0+\frac{1}{2})\theta-\pi/4]}}{\Delta/2-i(\theta+\theta_0)}\Big\}.\quad(69)$$

For $\theta_0\gg\bar{\Delta}/2$, the behavior of $|B(\theta)|^2$ around θ_0 is given approximately by

$$|B(\theta)|^2=\frac{4(2L_0+1)I_{L_0}{}^2}{\sin\theta}\frac{1}{(\theta-\theta_0)^2+(\Delta/2)^2}.\quad(70)$$

Expression (67) consists of two contributions: a smooth part, and an oscillatory interference term. The condition for damping of the oscillations is

$$\frac{\cosh^2[\delta\pi(\theta-\theta_0)]-\cos^2[\delta(\bar{\Delta}/2)\pi]}{\cosh^2[\delta\pi(\theta+\theta_0)]-\cos^2[\delta(\bar{\Delta}/2)\pi]}\ll1.\quad(71)$$

For neutron transfer reactions between complex nuclei, $\pi\delta\bar{\Delta}/2$ ($\delta\bar{\Delta}/2=\bar{\beta}\bar{d}$) is a small number and, for $\theta\sim\theta_0$, the last quotient in θ may be approximated by

$$[\pi\delta(\Delta/2)e^{-2\pi\delta\theta_0}]^2,\quad(72)$$

and the condition for damping of the oscillations reads

$$2\pi\delta\theta_0\gg1.\quad(73)$$

The last condition is approximately

$$4\pi\bar{\eta}(\bar{d}/\bar{R})\gg1.\quad(74)$$

Hence the condition for damping of the diffraction oscillations is essentially the same as the corresponding conditions[4,19] in the elastic scattering of charged particles with parameters $\bar{\eta}$, $\bar{d}$, $\bar{R}$. In many heavy-ion experiments this condition is well satisfied. The angular distribution around θ_0 is therefore given approximately by

$$\frac{d\sigma}{d\Omega}\propto\frac{1}{\sin\theta}\frac{1}{\cosh^2[\delta\pi(\theta-\theta_0)]-\cos^2[\delta(\bar{\Delta}/2)\pi]}.\quad(75)$$

It was pointed out by many authors[4,20] that it is physically more significant to consider

$$d\sigma/d\theta=2\pi\sin\theta d\sigma/d\Omega,\quad(76)$$

because thereby one extracts the $(\sin\theta)^{-1}$ dependence arising from the restriction of the reaction products to the scattering plane in the classical limit. For this reason we present the experimental data to be analyzed in Sec. IV in the form (76). From (75) we see that $d\sigma/d\theta$ has a symmetrical peak around θ_0 whose half-width satisfies

$$\sinh[\pi\delta(\theta_{1/2}-\theta_0)]=\sin(\pi\bar{\beta}\bar{d}).\quad(77)$$

For $\pi\bar{\beta}\bar{d}$ small an approximate solution of (77) is

$$\theta_{1/2}-\theta_0\sim\bar{\beta}\bar{d}/\delta\sim\bar{\beta}/\bar{k},\quad(78)$$

which coincides with half the width obtained for zero diffuseness.

At very small angles condition (71) is not satisfied and one expects an oscillatory diffraction pattern. This is not yet evident from the experimental angular distribution. On the other hand, the data are not accurate enough to rule out slight oscillatory structure at small angles. The experimental angular distribution does show smooth variation with scattering angle around θ_0 in accordance with prediction (75). Moreover, condition (1) is not satisfied for very small angles and one should not rely on prediction (75) for such angles.

[18] A. Dar, Weizmann Institute, October 1964 (unpublished).

[19] W. E. Frahn and R. H. Venter, Ann. Phys. **24**, 243 (1963).

[20] R. Kaufmann and R. Wolfgang, Phys. Rev. **121**, 206 (1961). See also Ref. 3.

(b) The Transfer Excitation Function

For energy above the Coulomb barrier, the transfer excitation function satisfies (41) with

$$S(E)=4\pi\sum_{0}^{\infty}(2l+1)|a_l|^2|I_l|^2. \tag{79}$$

One now introduces the asymptotic expression for I_l Eq. (27) into Eq. (42) and approximates summation over l by integration over classical distance of closest approach. For the R dependence of the reflection coefficients a_l, one assumes

$$a(R)=\{1+\exp[(\bar{R}_{aA}-\bar{R})/\bar{d}]\}^{-1}. \tag{80}$$

Since $a(R)\sim 0$ for $R<0$, one can formally extend the integration to minus infinity in order to obtain

$$S(E)=\frac{\pi^2c^2\bar{\eta}^2}{2\beta^2\bar{k}^4(\gamma^2+\xi^2)}\exp[-2\gamma+2(\gamma^2+\xi^2)^{1/2}-2\xi\phi]$$
$$\times\exp\left\{-\left[\frac{2(\gamma^2+\xi^2)^{1/2}}{\bar{\eta}}\right]\bar{k}\bar{R}_{aA}\right\}$$
$$\times\pi\bar{k}\bar{d}\bar{\Delta}(1-\bar{k}\bar{d}\bar{\Delta})\csc(\pi\bar{k}\bar{d}\Delta). \tag{81}$$

The sharp cutoff result may be obtained by letting d in the smooth cutoff factor tend to zero, i.e.,

$$\lim_{d\to 0}\pi\bar{k}d\Delta(1-\bar{k}\bar{d}\bar{\Delta})\csc(\pi\bar{k}\bar{d}\bar{\Delta})=1. \tag{82}$$

Since $\bar{k}\bar{d}\bar{\Delta}\sim\bar{\beta}\bar{d}$ for energy well above the Coulomb barrier, the smooth cutoff factor does not contribute any energy-dependent factor. For $\xi/\gamma\ll 1$, $S(E)$ reduces

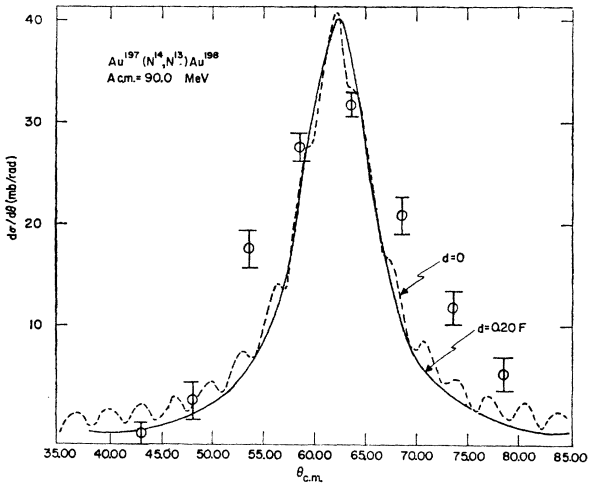

FIG. 1. Angular distribution $d\sigma/d\theta$ for the reaction Au^{197}-$(N^{14},N^{13})Au^{198}$. $E_{c.m.}=90$ MeV. The parameters of the theoretical curves are given in Table I.

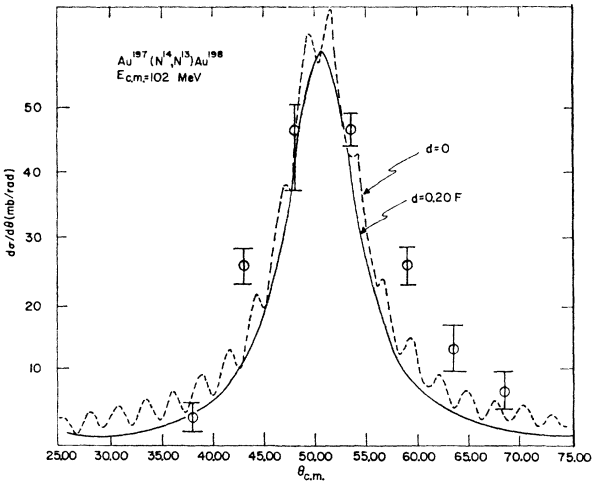

FIG. 2. Angular distribution $d\sigma/d\theta$ for the reaction Au^{197}-$(N^{14},N^{13})Au^{198}$. $E_{c.m.}=102$ MeV. The parameters of the theoretical curves are given in Table I.

to

$$S(E)\sim\frac{\pi^2c^2}{2\beta^4\bar{k}^2}e^{-\xi^2/\gamma}\exp(-2\bar{\beta}\bar{R}_{aA})$$
$$\times\pi\bar{\beta}\bar{d}(1-\bar{\beta}\bar{d})\csc(\pi\bar{\beta}\bar{d}). \tag{83}$$

IV. ANALYSIS OF EXPERIMENTAL DATA

A. Summary of Results

The final results for the differential cross section and excitation function, for cluster transfer reactions between complex nuclei, can now be summarized as follows:

The differential cross section is given by Eq. (14).

$$\frac{d\sigma}{d\Omega}=\frac{M_{bB}M_{aA}}{(2\pi\hbar^2)^2}\left(\frac{k_b}{k_a}\right)\frac{(2J_B+1)}{(2J_A+1)}|\bar{F}|^2|\bar{B}(\theta)|^2. \tag{84}$$

$\bar{F}$ is the angle-independent form factor as defined in Eq. (15), averaged over initial and final channels.

$$|\bar{F}|^2=4\pi\int j_{l_a}(i\beta r)V_{bc}(r)\chi_{l_a}(r)r^2dr$$
$$\times\int j_{l_B}(i\alpha r)V_{Ac}(r)\chi_{l_B}(r)r^2dr, \tag{85}$$

where V_{bc}, V_{Ac} are the interactions which bind c to the cores b and A, respectively. χ_{l_a}, χ_{l_B} are the radial wave functions for the relative motion of the core and the cluster c in particles a and B, respectively. j_l is the spherical Bessel function of order l. α and β are defined in Eqs. (11), (34), respectively.

For energy well below the Coulomb barrier and for nonidentical particles the angle-dependent factor,

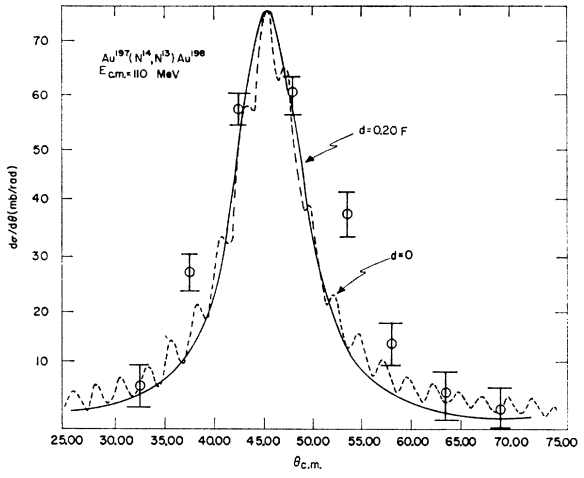

FIG. 3. Angular distribution $d\sigma/d\theta$ for the reaction Au^{197}-$(N^{14},N^{13})Au^{198}$. $E_{c.m.}=110$ MeV. The parameters of the theoretical curves are given in Table I.

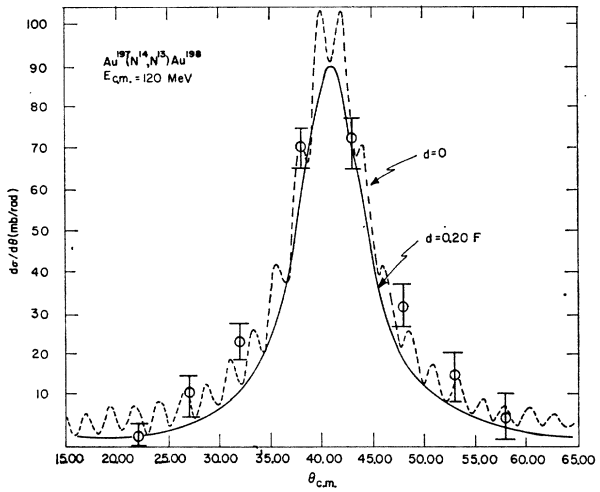

FIG. 4. Angular distribution $d\sigma/d\theta$ for the reaction Au^{197}-$(N^{14},N^{13})Au^{198}$. $E_{c.m.}=120$ MeV. The parameters of the theoretical curves are given in Table I.

$|\bar{B}(\theta)|^2$, is given by Eq. (32)

$$|\bar{B}(\theta)|^2=\frac{\pi^2\bar{\eta}^2\bar{c}^2e^{-\gamma_1-\gamma_2-\xi\phi_1-\xi\phi_2}}{2\alpha\beta\bar{k}^4[(\gamma_1^2+\xi^2)(\gamma_2^2+\xi^2)]^{1/4}}[\sin(\tfrac{1}{2}\theta)]^{-3}$$
$$\times\exp\{-[(\gamma_1^2+\xi^2)^{1/2}+(\gamma_2^2+\xi^2)^{1/2}]\csc(\tfrac{1}{2}\theta)\}, \quad (86)$$

where

$$\gamma_1=\bar{\eta}\beta/\bar{k}, \quad \gamma_2=\bar{\eta}\alpha/\bar{k}, \quad \tan\phi_1=\xi/\gamma_1, \quad \tan\phi_2=\xi/\gamma_2,$$

and with

$$\xi\approx-\frac{\bar{\eta}Q}{2(E)^{1/2}(E+Q)^{1/2}}. \quad (87)$$

For energy well above the Coulomb barrier, $B(\theta)$ is given by Eq. (66)

$$B(\theta)=2\pi\delta(2L_0+1)^{1/2}I_{L_0}(\sin\theta)^{-1/2}\{e^{i[(L_0+\frac{1}{2})\theta-\pi/4]}$$
$$\times\csc[\pi\delta\bar{\Delta}/2-i\pi\delta(\theta+\theta_0)]+e^{-i[(L_0+\frac{1}{2})\theta-\pi/4]}$$
$$\times\csc[\pi\delta\bar{\Delta}/2+i\pi\delta(\theta-\theta_0)]\}\exp(2i\sigma_{L_0}),$$

where

$$\bar{\Delta}=(\alpha+\beta)/\bar{k}. \quad (88)$$

$L_0\hbar$, and θ_0, are the angular momentum and the Rutherford scattering angle, respectively, which correspond to a grazing collision [Eqs. (57), (63)]. I_l is given by Eq. (27). δ is the diffuseness of the form factor [Eq. (56)] for the l dependence of the reflection coefficients. $|B(\theta)|^2$ is given by Eq. (67).

$$|B(\theta)|^2=4\pi^2\delta^2(2L_0+1)I_{L_0}{}^2\frac{1}{\sin\theta}\Bigg[\frac{1}{\cosh^2[\delta\pi(\theta-\theta_0)]-\cos^2[\delta(\bar{\Delta}/2)\pi]}+\frac{1}{\cosh^2[\delta\pi(\theta+\theta_0)]-\cos^2[\delta(\bar{\Delta}/2)\pi]}$$
$$+\frac{\cos[(2L_0+1)\theta-\pi/2][\cosh(2\pi\delta\theta_0-\cos(\pi\delta\bar{\Delta})\cosh(2\pi\delta\theta)]-\sin[(2L_0+1)\theta-\pi/2]\sin(\pi\delta\bar{\Delta})\sinh(2\pi\delta\theta)}{(\cosh^2[\delta\pi(\theta+\theta_0)]-\cos^2[\delta(\bar{\Delta}/2)\pi])(\cosh^2[\delta\pi(\theta-\theta_0)]-\cos^2[\delta(\bar{\Delta}/2)\pi])}\Bigg]. \quad (89)$$

For physical values of δ, $|B(\theta)|^2$ may be well approximated by

$$|B(\theta)|^2\approx4\pi^2\delta^2(2L_0+1)I_{L_0}{}^2\frac{1}{\sin\theta}\Bigg[\frac{1}{\cosh^2[\delta\pi(\theta-\theta_0)]-\cos^2[\delta(\bar{\Delta}/2)\pi])}\Bigg]. \quad (90)$$

For $\theta_0\gg\bar{\Delta}/2$, $B(\theta)$ behaves in the neighborhood of θ_0 like the "zero diffuseness amplitude" given by Eq. (70).

$$|B(\theta)|^2\approx\frac{4(2L_0+1)I_{L_0}{}^2}{\sin\theta}\frac{1}{(\theta-\theta_0)^2+(\bar{\Delta}/2)^2}. \quad (91)$$

The transfer excitation function is given by Eq. (41).

$$\sigma(E)=\frac{M_{aA}M_{bB}}{(2\pi\hbar^2)^2}\frac{(2J_B+1)}{(2J_A+1)}\frac{k_b}{k_a}|\bar{F}|^2S(E), \quad (92)$$

where

$$S(E)=\frac{\pi^2\bar{c}^2\bar{\eta}^2}{2\alpha\beta\bar{k}^4(\gamma_1^2+\xi^2)^{1/2}(\gamma_2^2+\xi^2)^{1/2}}$$
$$\times\exp[-\gamma_1-\gamma_2+(\gamma_1^2+\xi^2)^{1/2}$$
$$+(\gamma_2^2+\xi^2)^{1/2}-\xi\phi_1-\xi\phi_2]$$
$$\times M\exp[-(\gamma_1^2+\xi^2)^{1/2}k_aR_{aA}{}^{\min}/$$
$$\eta_a-(\gamma_2^2+\xi^2)^{1/2}k_bR_{bB}{}^{\min}/\eta_b]. \quad (93)$$

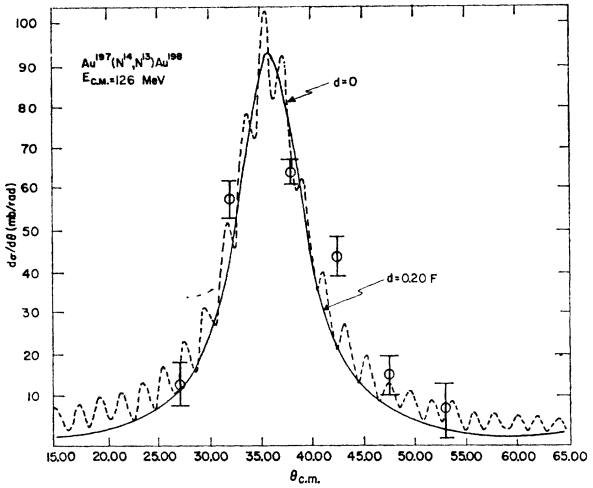

FIG. 5. Angular distribution $d\sigma/d\theta$ for the reaction $Au^{197}(N^{14},N^{13})Au^{198}$. $E_{c.m.}=126$ MeV. The parameters of the theoretical curves are given in Table I.

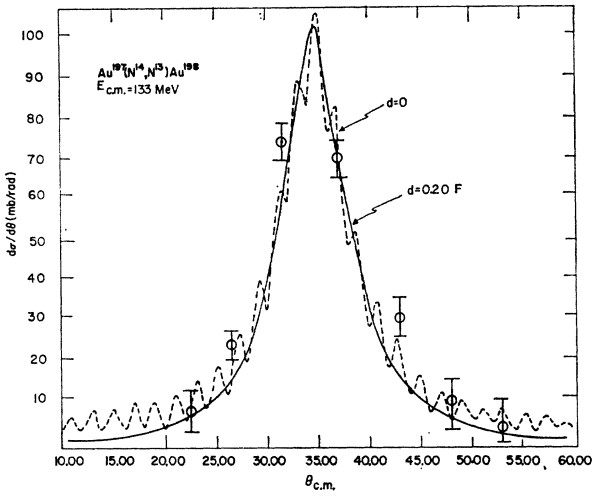

FIG. 6. Angular distribution $d\sigma/d\theta$ for the reaction $Au^{197}(N^{14},N^{13})Au^{198}$. $E_{c.m.}=133$ MeV. The parameters of the theoretical curves are given in Table I.

For energy well above the Coulomb barrier

$$R_{aA}{}^{\min}=R_{aA}\,,\quad R_{bB}{}^{\min}=R_{bB}\,,$$
$$M=\pi\bar{k}\bar{d}\bar{\Delta}(1-\bar{k}\bar{d}\bar{\Delta})\csc(\pi\bar{k}\bar{d}\bar{\Delta})\,, \tag{94}$$

where $\bar{d}$ is the diffuseness of the reflection coefficient's form factor in R space.

B. Comparison with Experimental Data

The theoretical predictions which are summarized in part A of the present section were compared with some of the experimental data. For energies well below the Coulomb barrier, our predictions coincide with the "tunneling-model" predictions that have been extensively applied to the experimental data. We, therefore, have concentrated on energies well above the Coulomb barrier.

The measured differential cross section, $d\sigma/d\Omega$, was converted to the form $d\sigma/d\theta$ by means of the identity

$$d\sigma/d\theta=2\pi\sin\theta d\sigma/d\Omega\,.$$

The angle θ_0 was chosen to be the angle at which $d\sigma/d\theta$ obtains its maximum value. The diffuseness $\bar{d}$ was kept at 0.20 F. This value is a little smaller than the average diffuseness[17] for medium energy, elastic scattering of heavy ions. It was chosen this way in order to account for the probably smaller diffuseness in the exit channels which characterizes the elastic scattering of unstable particles. In cases where it was not known whether the particles in the exit channel were excited or not, it was

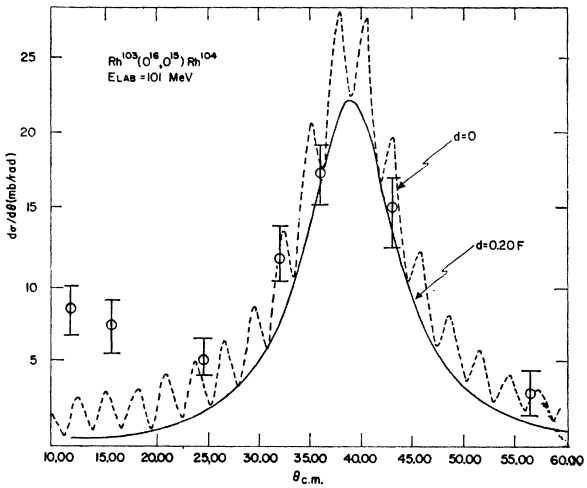

FIG. 7. Angular distribution $d\sigma/d\theta$ for the reaction $Rh^{103}(O^{16},O^{15})Rh^{104}$. $E_{c.m.}=87.42$ MeV. The parameters of the theoretical curves are given in Table I.

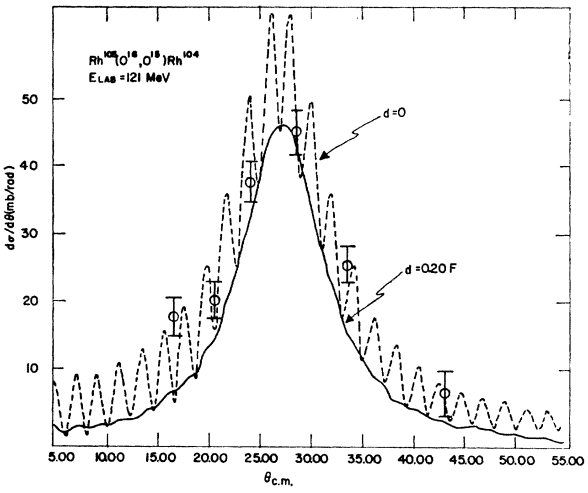

FIG. 8. Angular distribution $d\sigma/d\theta$ for the reaction $Rh^{103}(O^{16},O^{15})Rh^{104}$. $E_{c.m.}=104.73$ MeV. The parameters of the theoretical curves are given in Table I.

assumed that they emerged in their ground state. The theoretical predictions for each reaction were normalized once to give an over-all fit to all incident energies.

For comparison, the calculations were repeated for the case of zero diffuseness.

Four typical sets of cluster transfer distributions were analyzed:

(1) The data of McIntyre *et al.*[21] for the Au^{197}-$(N^{14},N^{13})Au^{198}$ reaction, at different projectile energies (heavy targets).

(2) The data of Kaufmann and Wolfgang[22] for the

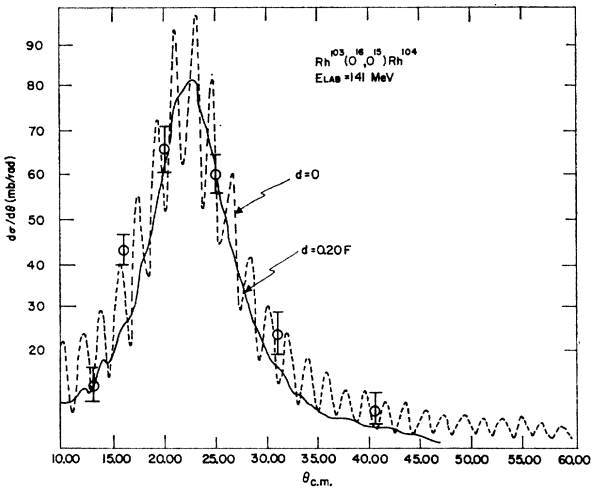

FIG. 9. Angular distribution $d\sigma/d\theta$ for the reaction Rh^{103}-$(O^{16},O^{15})Rh^{104}$. $E_{c.m.}=122.04$ MeV. The parameters of the theoretical curves are given in Table I.

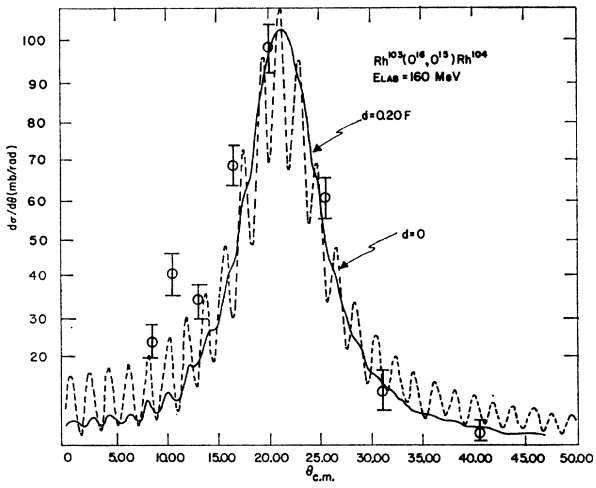

FIG. 10. Angular distribution $d\sigma/d\theta$ for the reaction Rh^{103}-$(O^{16},O^{15})Rh^{104}$. $E_{c.m.}=138.49$ MeV. The parameters of the theoretical curves are given in Table I.

[21] J. A. McIntyre, T. L. Watts, and F. C. Jobes, Phys. Rev. **119**, 1331 (1960); Ref. 1(f), p. 16.

[22] R. Kaufmann and R. Wolfgang, Phys. Rev. **121**, 1962 (1961); **121**, 206 (1961); Ref. 1(d), p. 30.

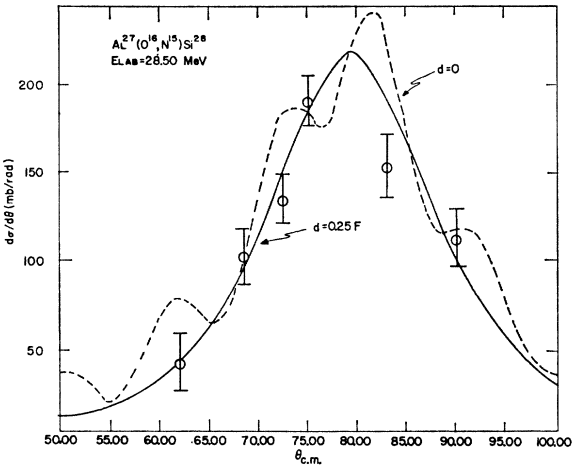

FIG. 11. Angular distribution $d\sigma/d\theta$ for the reaction Al^{27}-$(O^{16},N^{15})Si^{28}$. $E_{c.m.}=17.90$ MeV. The parameters of the theoretical curves are given in Table I.

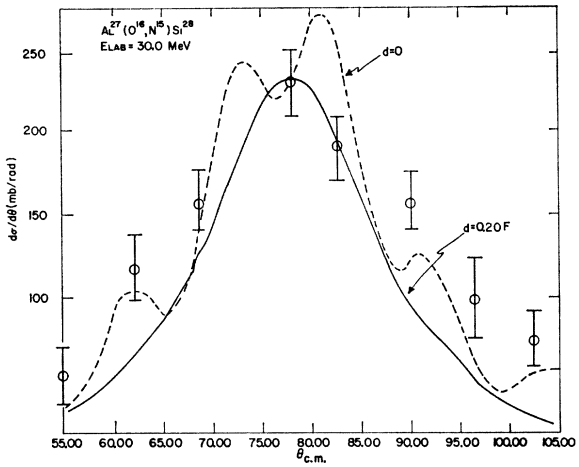

FIG. 12. Angular distribution $d\sigma/d\theta$ for the reaction Al^{27}-$(O^{16},N^{15})Si^{28}$. $E_{c.m.}=18.84$ MeV. The parameters of the theoretical curves are given in Table I.

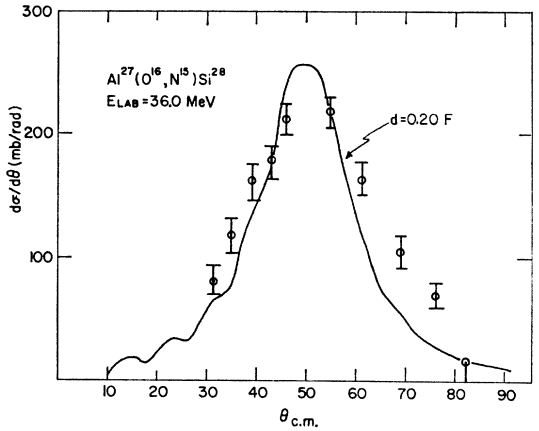

FIG. 13. Angular distribution $d\sigma/d\theta$ for the reaction Al^{27}-$(O^{16},N^{15})Si^{28*}$ $E_{c.m.}=22.60$ MeV. The parameters of the theoretical curves are given in Table I.

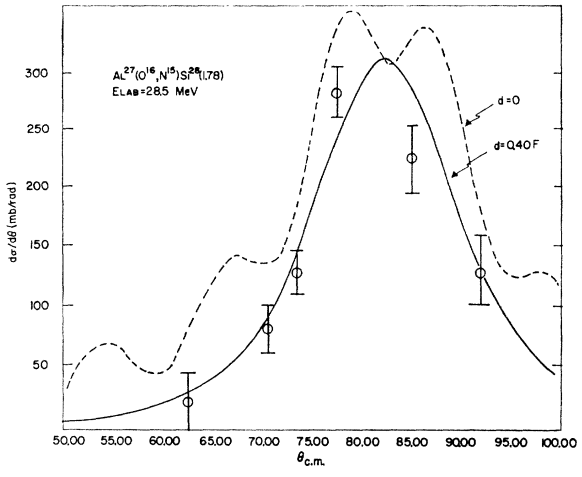

FIG. 14. Angular distribution $d\sigma/d\theta$ for the reaction Al^{27}-$(O^{16},N^{15})Si^{28*}$ (1.78 MeV). $E_{c.m.}=17.90$ MeV. The parameters of the theoretical curves are given in Table I.

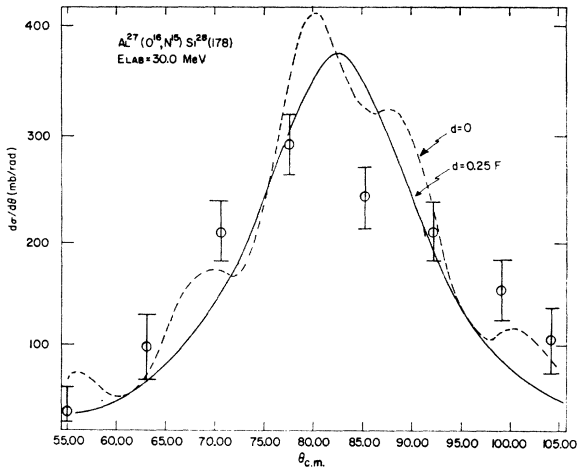

FIG. 15. Angular distribution $d\sigma/d\theta$ for the reaction Al^{27}-$(O^{16},N^{15})Si^{28*}$ (1.78 MeV). $E_{c.m.}=18.84$ MeV. The parameters of the theoretical curves are given in Table I.

$Rh^{103}(O^{16},O^{15})Rh^{104}$ reaction, at different projectile energies (medium weight targets).

(3) The data of Newman *et al.*[23] for the $Al(O^{16},N^{15})$-Si^{28*} (1.78 MeV) reactions at different projectile energies (light targets).

(4) The data of Sachs *et al.*[24] for the $C^{12}(B^{11},Be^{9})N^{14}$, $C^{12}(B^{10},Be^{9})N^{13}$ ground-state and excited-state reactions, at different projectile energies (small weight targets).

The results are shown in Figs. 1–21. The fits are summarized in Table I. They show the following characteristics:

(a) In most cases the fits are quite satisfactory.

(b) There is a clear trend for better fits towards higher energies. (Such a trend is consistent with the approximations, since they become more accurate at higher energies.)

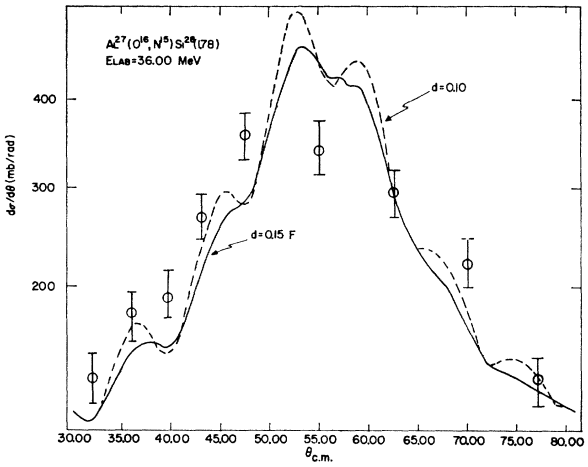

FIG. 16. Angular distribution $d\sigma/d\theta$ for the reaction Al^{27}-$(O^{16},N^{15})Si^{28*}$ (1.78 MeV). $E_{c.m.}=22.60$ MeV. The parameters of the theoretical curves are given in Table I.

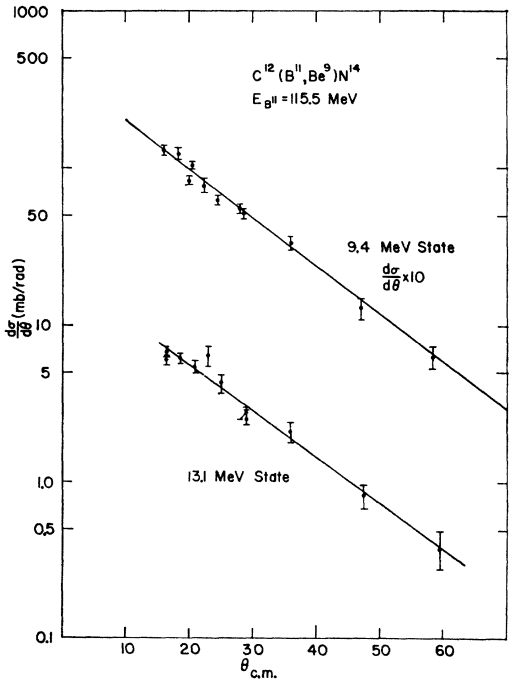

FIG. 17. Angular distribution $d\sigma/d\theta$ for the reactions C^{12}-$(B^{11},Be^{9})N^{14*}$ (9.4 MeV). $C^{12}(B^{11},Be^{9})N^{14*}$ (13.1 MeV) (deuteron transfer). $E_{c.m.}=60.3$ MeV. The parameters of the theoretical curves are given in Table I.

[23] E. Newman, K. S. Toth, and A. Zucker, Ref. 1(f), p. 143; Phys. Rev. **132**, 1720 (1963).

[24] M. Sachs, C. Chasman, and D. A. Bromley, Ref. 1(f), p. 90; Phys. Rev. **139**, B92 (1965).

(c) The experimental data favor finite diffuseness. (There is no evidence for a strong oscillatory behavior of the differential cross section, which characterizes zero diffuseness.)

(d) The diffuseness is largely energy-independent.

(e) The diffuseness tends to be somewhat smaller than the average surface diffuseness derived from heavy-ion elastic scattering.[17] (It probably accounts for the assumed smaller diffuseness for the elastic scattering of the unstable particles in the exit channel.)

(f) The "zero-diffuseness formula" [Eq. (91)] with

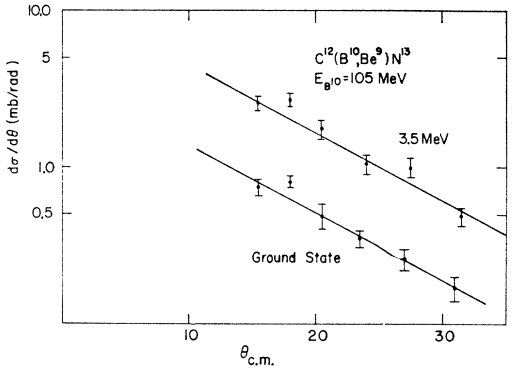

FIG. 18. Angular distribution $d\sigma/d\theta$ for the reactions $C^{12}(B^{10},Be^{9})N^{13}$, $C^{12}(B^{10},Be^{9})N^{13*}$ (3.5 MeV). $E_{c.m.}=57.3$ MeV. The parameters of the theoretical curves are given in Table I.

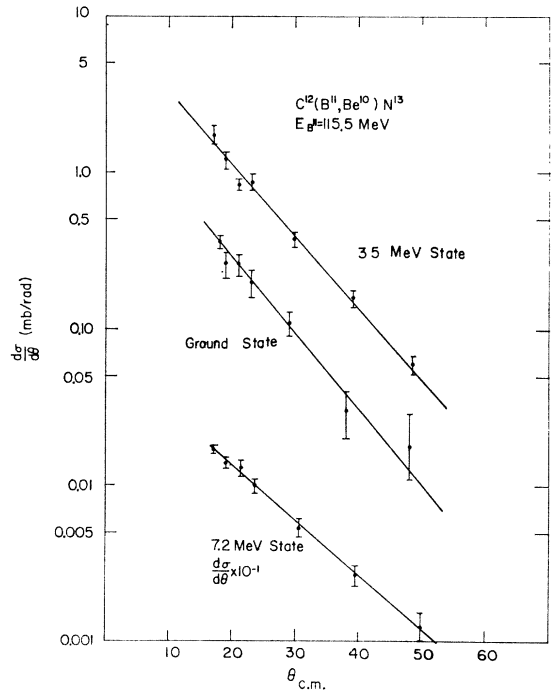

FIG. 19. Angular distribution $d\sigma/d\theta$ for the reactions $C^{12}(B^{11},Be^{10})N^{13}$, $C^{12}(B^{11},Be^{10})N^{13*}$ (3.5 MeV), $C^{12}(B^{11},Be^{10})N^{13*}$ (7.2 MeV). $E_{c.m.}=60.3$ MeV. The parameters of the theoretical curves are given in Table I.

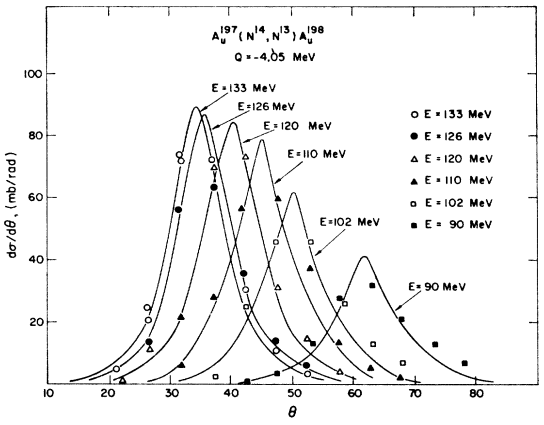

FIG. 20. Angular distribution $d\sigma/d\theta$ for the reaction $Au^{197}(N^{14},N^{13})Au^{198}$. Experimental points from J. A. McIntyre, T. L. Watts, and F. C. Jobes, Phys. Rev. **119**, 133 (1960). The theoretical curve was calculated from Eq. (91). The parameters are those given in Table I.

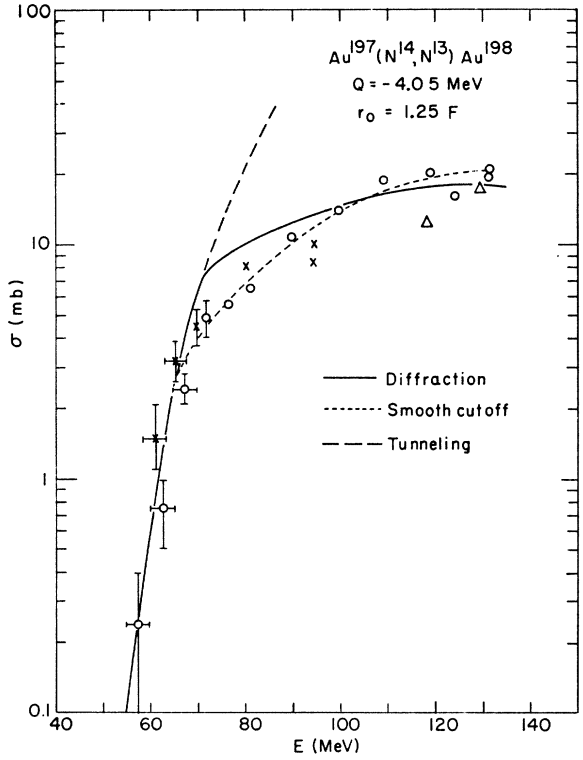

FIG. 21. Transfer excitation function plotted against c.m. energy. The circles, crosses, and triangles indicate results obtained on repeated experiments. The diffraction curve was calculated from Eq. (92). The smooth cutoff curve was calculated numerically from Eq. (79), where the parameters of the Saxon-Woods form factor for a_l were taken from Ref. 17.

the neglect of the interference term, proves to be a reliable interpolating formula in a small region around θ_0.

(g) The radius parameter r_0 is appreciably larger

TABLE I. Transfer reaction parameters.

Reaction	$E_{c.m.}$	$\bar{n}$	θ_0 (deg)	L_0	δ	R (F)	r_0 (F)	d (F)	Δ (deg)	Ref.
$Rh^{103}(O^{16},O^{15})Rh^{104}$	87.42	21.83	39.00	61.63	1.63	11.32	1.57	0.20	11.12	22
	104.73	20.01	27.00	83.36	1.73	12.59	1.75	0.20	10.34	
	122.04	18.59	22.40	93.88	1.84	12.64	1.76	0.20	9.54	
	138.49	17.48	21.20	93.43	1.96	11.71	1.63	0.20	8.94	
$Au^{197}(N^{14},N^{13})Au^{198}$	90.00	33.12	62.20	54.90	1.70	13.31	1.62	0.20	8.59	21
	102.00	31.07	50.70	65.57	1.72	13.31	1.62	0.20	8.48	
	110.00	29.89	45.50	71.29	1.75	13.25	1.61	0.20	8.31	
	120.00	28.60	41.00	76.49	1.80	13.04	1.59	0.20	8.05	
	126.00	27.90	37.00	83.38	1.83	13.36	1.63	0.20	7.95	
	133.00	27.14	34.70	86.87	1.87	13.26	1.61	0.20	7.78	
$Al^{27}(O^{16},N^{15})Si^{28}$	17.90	12.29	79.50	14.78	0.90	11.18	2.03	0.25	23.44	23
	18.84	11.96	78.00	14.76	0.74	10.68	1.94	0.20	23.02	
	22.60	10.85	50.50	21.07	0.72	10.82	1.96	0.20	22.94	
$Al^{27}(O^{16},N^{15})Si^{28*}(1.78)$	17.90	11.97	82.50	13.64	1.52	10.40	1.89	0.40	22.47	
	18.84	11.66	82.50	13.29	0.78	9.87	1.79	0.20	21.90	
	22.60	10.63	50.00	20.42	0.73	10.32	1.87	0.20	21.4	
$C^{12}(B^{11},Be^{9})N^{14*}(9.4)$	60.3	1.50						0.18		24
$C^{12}(B^{11},Be^{9})N^{14*}(13.1)$	60.3	1.53						0.18		
$C^{12}(B^{10},Be^{9})N^{13}$	57.3	1.43						0.24		
$C^{12}(B^{10},Be^{9})N^{13*}(3.5)$	57.3	1.45						0.24		
$C^{12}(B^{11},Be^{10})N^{13}$	60.3	1.47						0.23		
$C^{12}(B^{11},Be^{10})N^{13*}(3.5)$	60.3	1.49						0.23		
$C^{12}(B^{11},Be^{10})N^{13*}(7.2)$	60.3	1.53						0.19		

than the mean radius parameter obtained from heavy-ion elastic scattering.[17]

(h) The radius parameter r_0 is larger for the ground state than it is for the excited states.

CONCLUSIONS

This article presents a quantum-mechanical derivation for the tunneling-model predictions at energies below the Coulomb barrier. For energies well above the barrier the present work is a natural extension of the work of Frahn and Venter. A satisfactory simple picture for transfer reactions between complex nuclei is obtained. Simple closed-form expressions based on this picture prove to reproduce remarkably the experimental data. Deviations from our prediction may be attributed to more complicated mechanisms of reactions, such as reactions via resonant states, reactions via high-l boiling, compound-system reactions, etc.

ACKNOWLEDGMENTS

The author would like to thank Professor A. de-Shalit and Professor W. E. Frahn for fruitful discussions.